journal

J. Am. Ceram. Soc., 78 [4] 933–38 (1995)

Effect of Synthesis Techniques on Crystallite Size and Morphology of Lithium Aluminate

Luz María Carrera,† Jaime Jimenez-Becerril,† Pedro Bosch,†,‡ and Silvia Bulbulian†

Departamento de Química, Instituto Nacional de Investigaciones Nucleares, C. P. 11801, México, D.F.

Departamento de Química, Universidad Autónoma Metropolitana-Iztapalapa, C. P. 09340, México, D.F.

γ-$LiAlO_2$ is considered as a candidate tritium breeder material for fusion reactors because of its thermophysical, chemical, and mechanical stability at high temperatures and its favorable neutron irradiation behavior. Crystallite size and shape could, however, alter these features. In this study the mean crystallite size, the crystallite size distribution, and the morphology of γ-$LiAlO_2$ are correlated to the synthesis procedure. The characterization techniques were powder X-ray diffraction and scanning electron microscopy.

I. Introduction

THE future of nanophase ceramics is extremely bright but still largely uncharted. Several interesting and technologically important nanophase oxides have already been produced and some of their properties are now being elucidated.[1] While their mechanical properties have already received some scrutiny, largely directed toward an initial assessment of their durability, formability, and suitability for application, the importance of the width of the grain size distribution to the sinterability of nanophase ceramics needs to be considered further.[2]

In considering γ-$LiAlO_2$ as a candidate tritium breeder material for fusion reactors, researchers have generally been driven by a need to prepare a reproducible product.[3–5] Briec *et al.*[6] in in-pile irradiation experiments on samples of lithium aluminate provided tritium retention and release data, but as is the case for all tritium breeders, the interpretation of results was not straightforward. The results were not explained if only the kinetic contribution to the tritium inventory, diffusion, or mass transfer resistance at the solid–gas interface is considered. It was necessary to consider tritium adsorption at grain surfaces in order to explain that, at higher temperatures, small grain samples have a higher tritium inventory than samples with large grains.

Other authors have reported many different processes to produce lithium aluminate.[7–9] They have been able to obtain pure powders with good sintering properties, with various morphologies and different grain sizes. Alvani *et al.*[9] established a compromise between a near fully open porosity and grain sizes <1 μm to improve the thermomechanical and tritium release properties of γ-$LiAlO_2$. In previous studies,[10,11] we examined the synthesis of lithium aluminate and some of the characteristics of this material. The lithium aluminate was obtained using three procedures. It was found that the best synthesis technique involved the reaction of equimolar amounts of powdered γ-Al_2O_3 and Li_2CO_3, since it provided the product with the highest content of γ-$LiAlO_2$. After heating at 1000°C for 1 h, all the preparation techniques resulted in a mixture of γ-$LiAlO_2$ and $LiAl_5O_8$. The purpose of the present study is to correlate the preparation technique of lithium aluminate with the crystallite size distribution (CSD), the crystallite mean size (CMS), and the morphology of the lithium aluminate product.

II. Experimental Procedure

(1) *Preparation of the Lithium Aluminate*

Lithium aluminate powders were synthesized following three techniques described by the equations in this section. Although the powders were not stoichiometrically balanced, they showed the identified compounds in the X-ray diffraction data taken at 700° and 1000°C.[10]

The carbonate-reaction (Li_2CO_3/Al_2O_3) method involved the reaction of equimolar amounts of powdered γ-Al_2O_3 and Li_2CO_3; they were intimately mixed in acetone and air dried, and then the mixture was heated at 700°C for 3 h and at 1000°C for 1 h. The chemical equations describing this procedure (Li_2CO_3/Al_2O_3) are

$$Li_2CO_3 + \gamma\text{-}Al_2O_3 \xrightarrow[3\ h]{700^\circ C} \gamma\text{-}LiAlO_2 + LiAl_5O_8 + CO_2 + \text{amorphous material}$$

$$\gamma\text{-}LiAlO_2 + LiAl_5O_8 + CO_2 + \text{amorphous material} \xrightarrow[1\ h]{1000^\circ C} \gamma\text{-}LiAlO_2 + LiAl_5O_8$$

γ-$LiAlO_2$ in the second equation is assumed to come from the amorphous material in the first equation as it is known that $LiAlO_2$ heated at high temperature produces $LiAl_5O_8$.

In the lithium hydroxide/aluminum metal reaction (LiOH/Al) approach, an excess ($LiOH/Al_{ex}$) or an equimolar amount ($LiOH/Al_{eq}$) of metallic aluminum powder was dissolved in 1*M* LiOH solution. In the first case a gray powder of aluminum and aluminum oxides was formed. In the second case, when an equimolar amount of metallic aluminum powder was used, an almost transparent solution was obtained. In both cases the solids were separated by filtration and the lithium aluminate was precipitated by adjusting the pH of the solution with 1*N* NaOH solution to values between 11 and 11.5. The colloidal product obtained was washed in cold water, alcohol, and ether. The resulting product was dried in air at 400°C for 1 h, and then calcined at 700°C for 3 h and 1000°C for 1 h.

The chemical equations describing the ($LiOH/Al_{ex}$) procedure with an excess of metallic aluminum powder are

$$LiOH_{(aq)} + 2Al_{(s)} \xrightarrow{\text{filtration}} \begin{cases} \text{gray powders (aluminum and aluminum oxides)} \\ Li^+ + Al(OH)_4^- \quad \text{(solution)} \end{cases}$$

$$Li^+ + Al(OH)_4^- \xrightarrow[\text{filtration}]{\text{pH 11–11.5}} \begin{cases} \text{waste water} \\ \text{white powders } [LiAl_2(OH)_7 \cdot 2H_2O + Al(OH)_3] \end{cases}$$

$$\text{white powders} \xrightarrow[3\ h]{700^\circ C} \text{amorphous material}$$

$$\text{amorphous material} \xrightarrow[1\ h]{1000^\circ C} \gamma\text{-}LiAlO_2 + LiAl_5O_8 + \text{amorphous material}$$

P. K. Davies—contributing editor

Manuscript No. 193711. Received March 28, 1994; approved October 18, 1994.

The chemical equations describing the ($LiOH/Al_{eq}$) procedure with an equimolar amount of metallic aluminum powder is described by the following chemical equations:

$$LiOH_{(aq)} + Al_{(s)} \xrightarrow{\text{filtration}} \begin{cases} \rightarrow \text{white powders (aluminum oxides)} \\ \rightarrow Li^+ + Al(OH)_4^- \quad \text{(solution)} \end{cases}$$

$$Li^+ + Al(OH)_4^- \xrightarrow[\text{filtration}]{\text{pH 11–11.5}} \begin{cases} \rightarrow \text{waste water} \\ \rightarrow \text{white powders } [LiAl_2(OH)_7 \cdot 2H_2O + Al(OH)_3] \end{cases}$$

$$\text{white powders} \xrightarrow[3\text{ h}]{700^\circ C} LiAl_2(OH)_7 + \text{amorphous material}$$

$$\text{amorphous material} + LiAl_2(OH)_7 \xrightarrow[1\text{ h}]{1000^\circ C} \gamma\text{-}LiAlO_2 + LiAl_5O_8 + \text{amorphous material}$$

The difference between the two LiOH/Al preparations is only the starting aluminum content.

The sodium hydroxide/aluminum metal (NaOH/Al) method involved the dissolution of metallic aluminum in 1*M* NaOH solution. Aluminum was added in twice the stoichiometric amount. The soluble sodium aluminate was filtered in order to eliminate the insoluble material. Then colloidal lithium aluminate was formed, adding to the filtered solution 1*N* LiCl at a pH between 11 and 11.5. The resulting mixture was again filtered and the solid washed until chloride free. The final product was dried and calcined as in the second method. The following chemical equations describe this procedure:

$$NaOH_{(aq)} + 2Al \xrightarrow{\text{filtration}} \begin{cases} \rightarrow \text{white powders (aluminum oxide)} \\ \rightarrow NaAlO_{2(aq)} \end{cases}$$

$$NaAlO_{2(aq)} + LiCl_{(aq)} \xrightarrow[\text{filtration}]{\text{pH 11–11.5}} \begin{cases} \rightarrow \text{waste water} \\ \rightarrow \text{white powders (aluminum oxides)} \end{cases}$$

$$\text{white powders} \xrightarrow[3\text{ h}]{700^\circ C} \text{amorphous material}$$

$$\text{amorphous material} \xrightarrow[1\text{ h}]{1000^\circ C} \gamma\text{-}LiAlO_2 + LiAl_5O_8 + \text{amorphous material}$$

The samples were labeled with the initial compounds used for the synthesis procedure and then the calcination temperature written as a subindex. Therefore, sample $(LiOH/Al_{eq})_{1000}$ is the ceramic prepared by procedure ($LiOH/Al_{eq}$) calcined at 1000°C.

(2) Crystallite Size Distribution

A Siemens D500 diffractometer coupled to a copper anode X-ray tube was used for X-ray diffraction analysis. The K_α^- wavelength was selected with a diffracted-beam monochromator. In the diffraction patterns, γ-$LiAlO_2$ and $LiAl_5O_8$ were identified using the JCPDS cards 18-714 and 17-573, respectively. From the areas under the diffraction peaks, the relative amounts of each compound were estimated. In the previous work[10] the method of calculating the area under the peaks had a 10% error (the papers under the peaks were cut and weighed); in this work these areas were analytically measured and the error diminished to less than 2%. As no internal standard was introduced, the X-ray absorption for each compound was assumed to be the same.

To study the crystallite size in γ-$LiAlO_2$ the (200) and (102) peaks were chosen as they were well-defined and independent. For $LiAl_5O_8$ the (311) and (220) peaks were chosen. The crystallite size distribution (CSD) was determined from the profile of these peaks with the XTL-SIZE computer program by Bonetto *et al.*,[12] which employs an indirect Fourier transform for analysis. The program determines the crystal size distribution in a direction perpendicular to an (*hkl*) crystal plane, from the corresponding digitalized XRD peak. The program is based on an information theory approach devised by Alvarez *et al.*[13] which considers that every diffraction peak can be described by means of a size distribution function and the number of scattering centers in the considered plane. Therefore, the crystallite size distribution for γ-$LiAlO_2$ was compared with the crystallite size distribution of $LiAl_5O_8$. The crystallite mean size (CMS) was also determined from the peak width using the Debye–Scherrer equation.[14]

If a crystallite size distribution is bimodal or trimodal, then the crystallite mean size value may be misleading. The cristallite size distribution is a histogram which describes the probability of finding a particle of a given size. The relative number of particles may be estimated from the area under the distribution curve and the area of the peak of interest. In this way, the relative amount of particles whose size is comprised between the two extreme values of the distribution peak may be obtained. Of course, the total area under the crystallite size distribution is related to the crystallite mean size and should agree with the crystallite mean size determined by the Debye–Scherrer equation. Lastly, it is important to remember that very small crystallites (<2 nm) produce X-reflections below the background level. Hence, in the crystallite size distribution, peaks located at diameters less than 3 nm will not be discussed.

(3) Morphology of the Lithium Aluminate Crystals

A Jeol JSM-T20 scanning electron microscope was used to determine the sample morphology. All samples were covered with a gold thin film using a JEOL (JFC-1100) fine coat ion sputter, so as to make the materials electrically conductive.

III. Results

As determined by X-ray diffraction, Table I shows the various lithium aluminate compounds present in the heated samples at 700° and 1000°C. Table II summarizes the features of the crystallite size distributions of γ-$LiAlO_2$ and $LiAl_5O_8$ in samples (Li_2CO_3/Al_2O_3), (LiOH/Al), and (NaOH/Al) all heated at 1000°C and in the [200] direction. All samples have a first peak whose maximum is at approximately 0.5 nm. This peak may not have a physical significance as it goes beyond the expected resolution of the method and therefore it is not included in Table II. The crystallite mean size, the location of the distribution peak maxima, the distribution peak widths at the base, as well as the relative number of particles are reported. The total number of particles was assumed to be proportional to the total area under the distribution curve, and, hence, the relative number of particles was estimated as the fraction of the area under the distribution curve.

Figures 1(A) and (B) show the temperature effect on the crystallite size distribution of γ-$LiAlO_2$, samples $(Li_2CO_3/Al_2O_3)_{700}$ and $(Li_2CO_3/Al_2O_3)_{1000}$, in the (200) and (102) crystallographic directions, respectively. The analogous effect for $LiAl_5O_8$ is shown in Figs. 1(C) and (D) for the (220) and (311) crystallographic directions. Samples $(LiOH/Al)_{700}$ and $(NaOH/Al)_{700}$ were noncrystalline materials.

Figure 2 shows the synthesized aluminate micrographs; (A) and (B) correspond to samples $(Li_2CO_3/Al_2O_3)_{1000}$ and $(Li_2CO_3/Al_2O_3)_{700}$, respectively, and (C) corresponds to sample $(LiOH/Al_{eq})_{1000}$.

Table I. Sample Composition

Sample	Calcination temperature (°C)	Composition (wt%)			
		γ-$LiAlO_2$	$LiAl_5O_8$	$LiAl_2(OH)_7$	Amorphous compound
Li_2CO_3/Al_2O_3	700	88	4		8
	1000	96	4		
$(LiOH/Al_{ex})$	700				100
	1000	49	36		15
$(LiOH/Al_{eq})$	700			67	33
	1000	30	20		50
NaOH/Al	700				100
	1000	26	41		33

Table II. Crystallite Size Distribution of γ-$LiAlO_2$ and $LiAl_5O_8$ According to the Synthesis Method

Sample	Compounds	CMS (nm)†	Peak position CSD (nm)‡	Peak width CSD (nm)‡	RNP (%)§
Li_2CO_3/Al_2O_3	γ-$LiAlO_2$	32.0	22.0	7.0	26.2
	γ-$LiAlO_2$	32.0	44.0	8.0	53.5
	$LiAl_5O_8$	20.5	26.0	6.5	8.9
($LiOH/Al_{ex}$)	γ-$LiAlO_2$	19.0	23.0	11.0	41.4
	$LiAl_5O_8$	18.0	12.0	9.5	11.2
	$LiAl_5O_8$	18.0	25.0	11.0	20.6
($LiOH/Al_{eq}$)	γ-$LiAlO_2$	19.0	20.0	13.5	22.8
	γ-$LiAlO_2$	19.0	27.5	5.5	2.9
	$LiAl_5O_8$	19.0	13.0	9.5	6.5
	$LiAl_5O_8$	19.0	25.0	11.0	12.3
NaOH/Al	γ-$LiAlO_2$	29.0	30.0	9.5	21.2
	$LiAl_5O_8$	10.5	10.0	4.5	8.1
	$LiAl_5O_8$	10.5	21.0	2.0	2.1

†Crystallite mean size. ‡Crystal size distribution. §Relative number of particles.

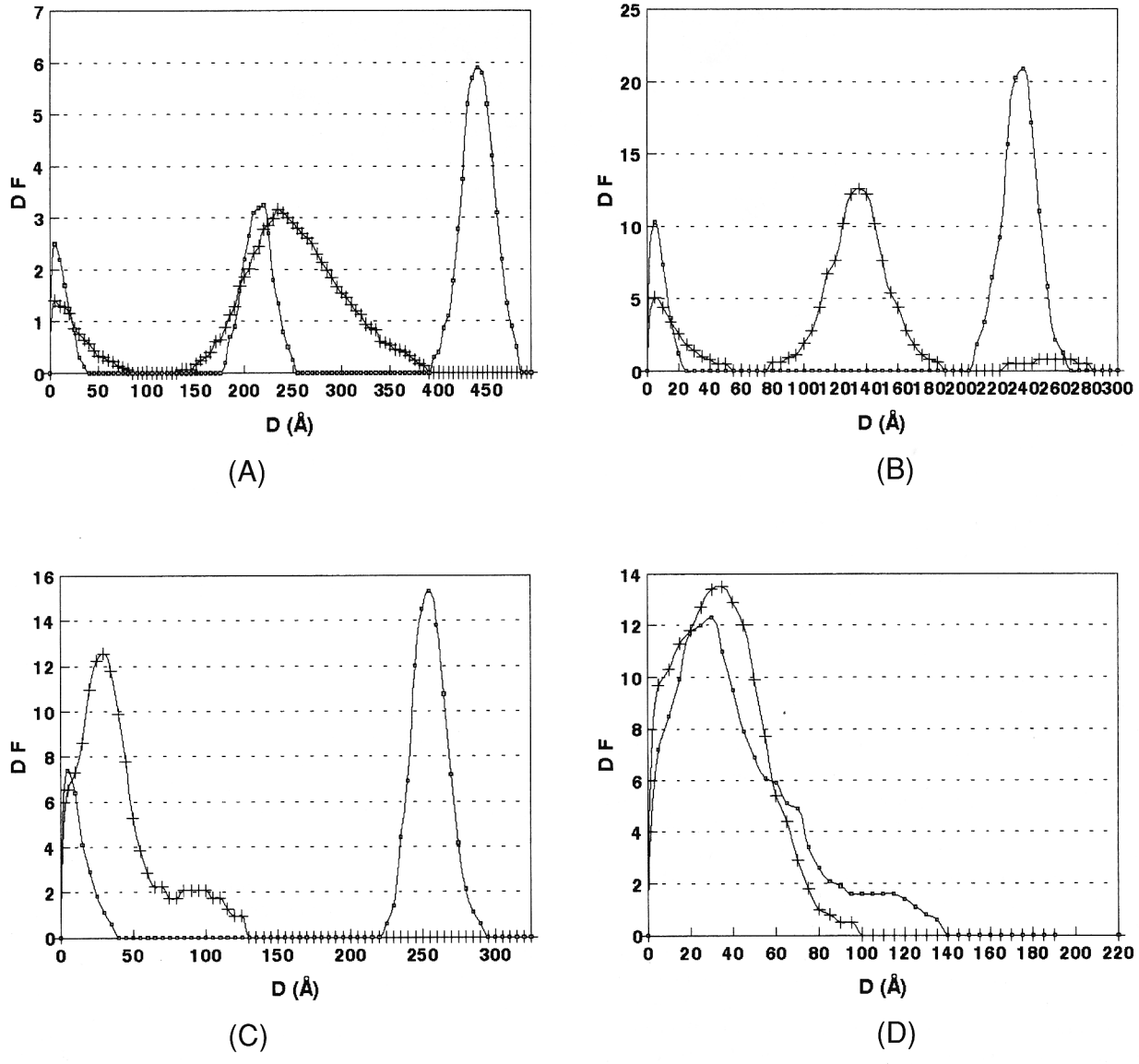

Fig. 1. Thermal effect on the crystal size distribution of lithium aluminate prepared by the (Li_2CO_3/Al_2O_3) method. All of the plots represent the distribution function (DF) versus the crystallite diameter (D) for 1000° (□) and 700°C (+). γ-$LiAlO_2$ in (200) direction (A) and in (102) direction (B). $LiAl_5O_8$ in (311) direction (C) and (220) direction (D).

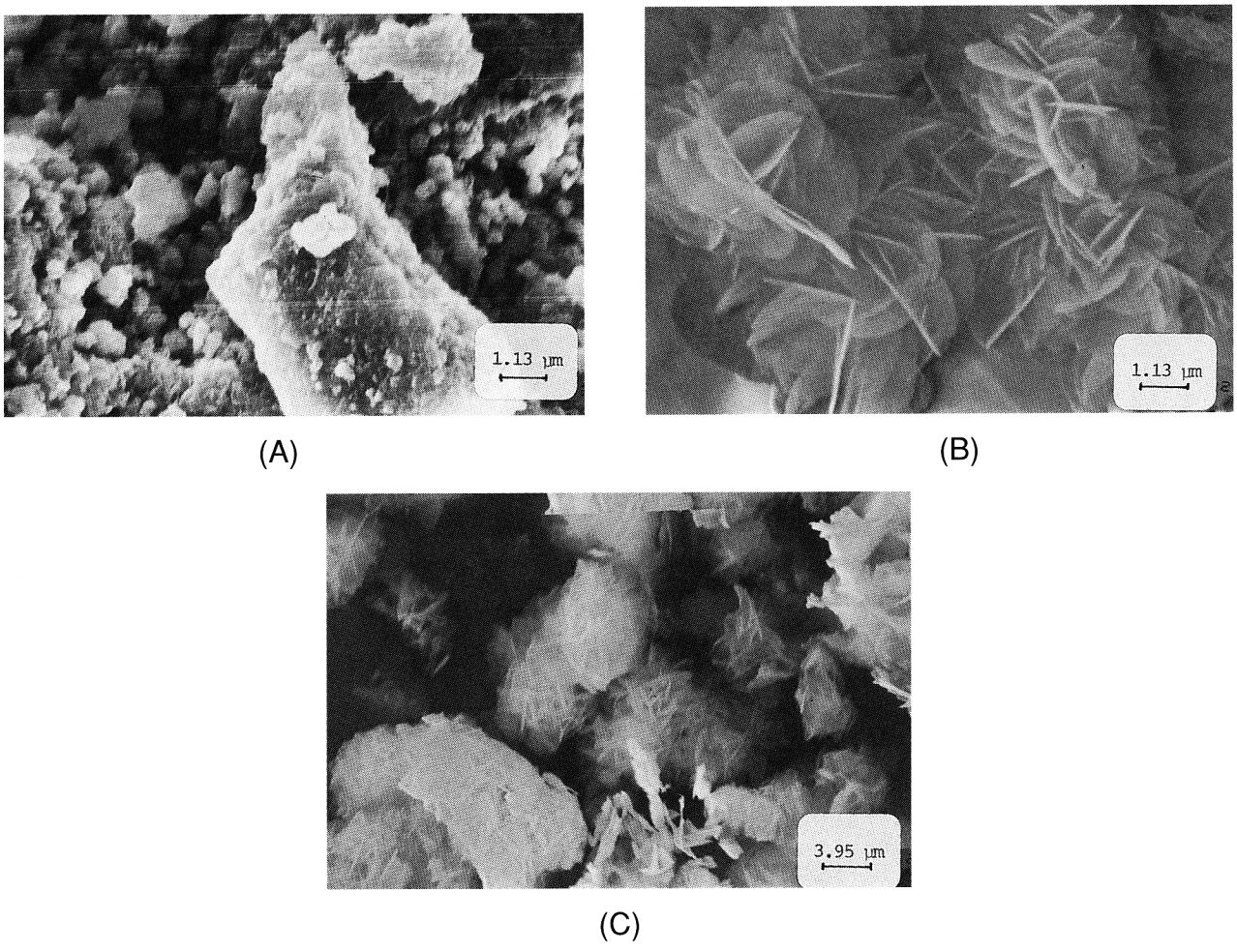

Fig. 2. Morphology of lithium aluminates: (A) sample $(Li_2CO_3/Al_2O_3)_{1000}$; (B) sample $(Li_2CO_3/Al_2O_3)_{700}$; (C) sample $(LiOH/Al)eq_{1000}$.

IV. Discussion

(1) Sintering Behavior

(A) Crystal Growth Mechanisms: To discuss the sintering behavior of all γ-$LiAlO_2$ preparations, a review of the crystal growth mechanisms as proposed in the bibliography is presented.[15–17] In a first step the lithium aluminate nuclei grow from a solution. There must be a transfer of atoms back and forth from the ordered crystal nuclei into the disordered liquid such that more atoms join the growing crystal. The crystallinity of the solid often imposes certain restraints on the overall growth process. In a second step, the recrystallization process, the original crystals are thermally treated, and the crystals grow in spite of neighbor small crystals. During thermal treatment, surface and bulk atoms become mobile at temperatures of about one third and one half of the melting point, respectively.

Two mechanisms have been proposed to explain crystallite growth.[15] The first one is crystallite migration. Small crystallites have a large fraction of surface atoms, mobile at temperatures lower than the bulk atoms. Therefore, a shape modification results. This mobility produces coalescence.

The second mechanism is interparticle transport of atoms from small to large crystallites. Yokoyama and Sekerka[16] have studied the combined effect of anisotropic surface tension and interface kinetics on pattern formation during the growth of two-dimensional crystals under conditions such that the growth is governed by interfacial processes. They classify crystal growth into three groups. The first one includes spherically growing particles characterized by a homogeneous crystal surface tension. The second comprises filamentous particles whose growth is due to a high local surface tension. Finally, the third group is formed by crystals growing irregularly with no preferred direction; this growth is explained by the presence of an inhomogeneous surface tension.

From the study of anhydrite crystals, Aquilano *et al.*[17] have obtained the critical mechanisms correlating the crystalline structure and the growth pattern. They proposed that the inhomogeneous surface tension is due to the atomic density in the crystallographic plane surface. Therefore, this second mechanism can be attributed to a driving force due to the larger free energy of the smaller crystallites. Therefore, small crystallites evaporate easily and condensation occurs on larger crystallites.

(B) Sample (Li_2CO_3/Al_2O_3): In the (Li_2CO_3/Al_2O_3) procedure, lithium aluminate was obtained through a dry process, heating a mixture of γ-Al_2O_3 and Li_2CO_3. At 700°C, crystalline γ-$LiAlO_2$ (88%) and $LiAl_5O_8$ (4%) were obtained. On heating this sample at 1000°C, the amount of crystallized γ-$LiAlO_2$ increased whereas the crystalline $LiAl_5O_8$ remained constant. Therefore, we have assumed that γ-$LiAlO_2$ is formed from the amorphous material.

When the γ-$LiAlO_2$ and $LiAl_5O_8$ crystallite sizes (32.0 and 20.5 nm) are compared, it is found that the γ-$LiAlO_2$ grain size is approximately 1.5 times larger than the $LiAl_5O_8$ grain size (see Table II). It appears that the sintering mechanism was different for each compound. The crystallite size distribution of γ-$LiAlO_2$ in the (200) direction of the $(Li_2CO_3/Al_2O_3)_{700}$ sample is presented in Fig. 1. A single very wide peak which corresponds to crystallite sizes from 15.0 to 40.0 nm is presented in Fig. 1(A). The curve corresponding to sample $(Li_2CO_3/Al_2O_3)_{1000}$ presents two main peaks located at 22.0 and 44.0 nm; these crystal size values are related by a factor of 2. Therefore, the larger crystals must have been formed by the addition of successive layers, each 22.0 nm thick.

Instead, the crystallite size distribution of $LiAl_5O_8$, (311) direction (Fig. 1(C)), in sample $(Li_2CO_3/Al_2O_3)_{700}$, presents only one main peak whose maximum is located at 3.5 nm. The peak is very broad and has a clear shoulder from diameters (D) ≈5.0 nm to ≈12.5 nm. This peak fades away in the 1000°C-treated sample whose particle size distribution shows only one clear peak from 22.5 to 29.0 nm whose maximum is at 26.0 nm. It seems, then, that $LiAl_5O_8$ in sample (Li_2CO_3/Al_2O_3), when heated, sinters but the large particles are not formed by packing the monocrystals.

The observed behavior is in agreement with the theoretical crystal growth mechanisms previously presented. The crystallite migration model seems, indeed, to explain the crystallite sizes observed in the $(Li_2CO_3/Al_2O_3)_{1000}$ sample for γ-$LiAlO_2$. The crystals are packed by coalescence in the direction [102], as proposed by Aquilano *et al.*[17] The plane (102) indeed has a low crystallographic density. But $LiAl_5O_8$ growth may happen by any of the two mechanisms or both, as there is no clear correlation between the 700°- and 1000°C-treated samples. These mechanisms may point the way to possible synthesis modifications.

The comparison between Figs. 1(A) and (B) shows that the shape of the γ-$LiAlO_2$ crystallites is larger in the (200) direction, 23.0 nm, than in the (102) direction, 13.0 nm, for the $(Li_2CO_3/Al_2O_3)_{700}$ sample; therefore, the crystallites look like thin sheets. For sample $(Li_2CO_3/Al_2O_3)_{1000}$ this relationship is similar, 44.0 and 22.0 nm for the (200) and (102) directions, respectively. Therefore, the temperature increase does not alter the shape of the crystallites. This shape has been described by Yokoyama and Sekerka,[16] and it has been attributed to growth due to an inhomogeneous surface tension.

For $LiAl_5O_8$ in sample $(Li_2CO_3/Al_2O_3)_{700}$, crystallites have similar sizes, 4.0 nm (Fig. 1(C)) and 4.5 nm (Fig. 1(D)) in the (311) and (220) directions, respectively. Their shape can be approximated to a sphere when heated $(Li_2CO_3/Al_2O_3)_{1000}$; the (200) direction (Fig. 1(D)) is not affected but the crystals grow in the (311) direction (Fig. 1(C)). Hence, while the morphology is at 700°C close to a sphere, it turns out to be elliptical if the sample is treated at 1000°C. The corresponding homogeneous surface tension[16] seems to be fairly stable with temperature.

(C) Sample (LiOH/Al): The $(LiOH/Al_{ex})_{700}$ procedure produces a mixture of amorphous compounds, probably several aluminates. Most of these amorphous compounds were transformed at 1000°C to crystalline γ-$LiAlO_2$ (50%) and $LiAl_5O_8$ (36%). If the $(LiOH/Al_{eq})_{700}$ method is followed, 67 wt% of $LiAl_2(OH)_2$ is formed. If sample $(LiOH/Al_{eq})_{700}$ is heated at 1000°C, 30% crystallizes as γ-$LiAlO_2$ and 21% as $LiAl_5O_8$. In this case $LiAl_5O_8$ was less than in the previous $(LiOH/Al_{ex})$ case where more aluminum was utilized in the preparation technique. However, in both the $(LiOH/Al_{ex})$ and $(LiOH/Al_{eq})$ cases the γ-$LiAlO_2$/$LiAl_5O_8$ ratio of the compounds produced is very similar.

Crystallite size distributions of samples $(LiOH/Al_{ex})$ and $(LiOH/Al_{eq})$ are very similar to each other. In both cases γ-$LiAlO_2$ has a main peak located at around 21.5 nm, and also in both cases, $(LiOH/Al_{ex})$ and $(LiOH/Al_{eq})$ samples, $LiAl_5O_8$ has two main peaks with very similar peak positions around 25.0 nm. When lithium aluminate is formed by the dissolution of aluminum powder in a solution of LiOH, then its formation process is very similar in both cases, even though they have been formed with different amounts of metallic aluminum and the intermediate processes are different. The crystallite mean sizes of γ-$LiAlO_2$ and $LiAl_5O_8$ in both samples $(LiOH/Al_{ex})$ and $(LiOH/Al_{eq})$ are very similar around 19.0 nm.

The crystallite size distribution of γ-$LiAlO_2$ in both samples $(LiOH/Al_{ex})$ and $(LiOH/Al_{eq})$ has one main peak (maximum around 23.0 nm), but the crystallite size distribution of $LiAl_5O_8$ has two main peaks whose maxima are located at approximately 12.5 and 25.0 nm. We have to conclude, as in sample $(Li_2CO_3/Al_2O_3)_{1000}$, that in this case $LiAl_5O_8$ large crystals seem to be built by coalescence of layers of 12.5 nm. The $(LiOH/Al_{eq})$ sample has a distribution with a main peak for γ-$LiAlO_2$ (mean size 19.0 nm) and two main peaks for $LiAl_5O_8$ (mean size 19.0 nm).

(D) Sample NaOH/Al: The sample prepared by the (NaOH/Al) method is constituted of compounds with one main peak in the crystallite size distribution (30.0 nm) for γ-$LiAlO_2$ and two main peaks (10.0 and 23.0 nm for $LiAl_5O_8$.

(2) Morphology of the Lithium Aluminate Crystals

Figure 2 corresponds to micrographs of samples $(Li_2CO_3/Al_2O_3)_{1000}$ (A) and $(Li_2CO_3/Al_2O_3)_{700}$ (B). The thickness of the crystallite is 20.4 and 12.4 nm for samples $(Li_2CO_3/Al_2O_3)_{1000}$ and $(Li_2CO_3/Al_2O_3)_{700}$, respectively. These values are similar to those determined by X-ray diffraction in the (102) direction. Moreover, both micrographs confirm that the crystallite shape is laminar; the crystals look like flakes. Figure 2(C) corresponds to sample $(LiOH/Al_{eq})_{1000}$. Figures 2(C) and (B) show that the shapes of the crystallites are similar, but the $(LiOH/Al_{eq})$ sample crystallites are smaller. Therefore, the (Li_2CO_3/Al_2O_3) method provided the largest crystals. Hence, if large and well-grown crystals are needed, the best method to prepare γ-$LiAlO_2$ is the $(Li_2CO_3/Al_2O_3)_{1000}$. If they have to be small, the $(LiOH/Al)_{1000}$ method is recommended.

(3) Crystallinity

In the (Li_2CO_3/Al_2O_3) method, samples heated at 700°C had 8% of amorphous material and 4% of $LiAl_5O_8$, but in 1000°C-treated material very little amorphous material is found and $LiAl_5O_8$ remains constant. The amount of γ-$LiAlO_2$ is 88% at 700°C and 96% at 1000°C; hence amorphous material has crystallized, with temperature, as γ-$LiAlO_2$. This mechanism is different from the (LiOH/Al) and (NaOH/Al) syntheses mainly because crystallinity in them is attained only after heating at 1000°C and the amount of $LiAl_5O_8$ is considerably higher than in the (Li_2CO_3/Al_2O_3) method.

V. Conclusions

In the (Li_2CO_3/Al_2O_3) method, γ-$LiAlO_2$ crystals grow by coalescence; such is not the case if the (LiOH/Al) synthesis is followed, where only one type of crystal is formed. However, $LiAl_5O_8$ crystals are formed by coalescence in sample (LiOH/Al) but not in sample (Li_2CO_3/Al_2O_3). Therefore, the morphology of crystals and the crystal growth can be controlled using the different synthesis methods. Crystal growth definitely depended on the synthesis procedure.

Acknowledgments: We thank the technicians of the Chemistry Department (ININ) for their help in the laboratory, and V. H. Lara (UAM) for technical help in the X-ray diffraction measurements.

References

[1]D. Vollath, H. Wedemeyer, and E. Gunther, "Improved Methods for Fabrication of Lithium Silicates," *J. Nucl. Mater.*, **133–134**, 221 (1985).

[2]J. A. Eastman, Y. X. Liao, A. Narayanasamy, and R. W. Siegel; pp. 90–135 in *Processing Science of Advanced Ceramics*, Vol. 155. Edited by I. A. Aksay, G. L. McVay, and D. R. Ulrich. Materials Research Society, Pittsburgh, PA, 1989.

[3]C. E. Johnson, K. R. Kummerer, and E. Roth, "Ceramic Breeder Materials," *J. Nucl. Mater.*, **155–157**, 188 (1988).

[4]J. P. Kopasz, C. A. Seils, and C. E. Johnson, "Tritium Release from Lithium Aluminate: Can It Be Improved?," *J. Nucl. Mater.*, **191–194**, 231 (1992).

[5]N. Roux, C. Johnson, and K. Noda, "Properties and Performance of Tritium Breeding Ceramics," *J. Nucl. Mater.*, **191–194**, 15 (1992).

[6]M. Briec, J. J. Abassin, M. Masson, E. Roth, P. Sciers, and H. Werle, "In-Pile Tritium Extraction from Samples of Lithium Aluminate," *J. Nucl. Mater.*, **155–157**, 549 (1988).

[7]S. Casadio, C. Alvani, C. Ciavola, and P. Cigna, "Fabrication and Physicochemical Characterization of $LiAlO_2$ Targets for In-Pile Test of Ceramic Breeder Materials," *Fusion React. Des. Technol.*, **2**, 421 (1987).

[8]C. Alvani, S. Casadio, L. Contursi, and R. Fava, "Gamma Lithium Aluminate Fabrication by Microwave Heating Process"; p. 3087 in *Ceramics Today—Tomorrow's Ceramics*. Edited by P. Vicenzini. Elsevier Science Publishers, Amsterdam, Netherlands, 1991.

[9]C. Alvani and S. Casadio, "Ceramics Process versus Property Optimization of Lithium Aluminate as Tritium Breeder Material"; p. 3069 in *Ceramics Today—Tomorrow's Ceramics*. Edited by P. Vicenzini. Elsevier Science Publishers, Amsterdam, Netherlands, 1991.

[10]J. Jiménez-Becerril, P. Bosch, and S. Bulbulian, "Synthesis and Characterization of γ-$LiAlO_2$," *J. Nucl. Mater.*, **185**, 304 (1991).

[11]J. Jiménez-Becerril, P. Bosch, and S. Bulbulian, "^{18}F Presence in Neutron-Irradiated γ-$LiAlO_2$," *J. Nucl. Mater.*, **189**, 233 (1992).
[12]R. Bonetto, H. Viturro, and A. Alvarez, "XTL–SIZE: A Computer Program for Crystal-Size-Distribution Calculation from X-Ray Diffraction Line Broadening," *J. Appl. Crystallogr.*, **23**, 136 (1990).
[13]A. G. Alvarez, R. D. Bonetto, and D. M. A. Guérin, "Statistical Inference, Size Distributions and Peak Broadening in Finite Crystals," *Powder Diffr.*, **2**, 220 (1987).
[14]H. P. Klug and L. E. Alexander, *X-ray Diffraction Procedures*. Wiley, New York, 1974.
[15]J. T. Richardson, *Principles of Catalyst Development*. Plenum Press, New York, 1989.
[16]E. Yokoyama and R. F. Sekerka, "A Numerical Study of the Combined Effect of Anisotropic Surface Tension and Interface Kinetics on Pattern Formation During the Growth of Two-Dimensional Crystals," *J. Cryst. Growth*, **125**, 389 (1992).
[17]D. Aquilano, M. Rubbo, M. Catti, A. Pavese, and P. Ugliengo, "Theoretical Equilibrium and Growth Morphology of Anhydrite ($CaSO_4$) Crystals," *J. Cryst. Growth*, **125**, 519 (1992). □